Vibrational Spectroscopic Studies of the Attachment Chemistry for Zirconium Phosphonate Multilayers at Gold and Germanium Surfaces

Brian L. Frey, Dennis G. Hanken, and Robert M. Corn*

Department of Chemistry, University of Wisconsin—Madison, 1101 University Avenue, Madison, Wisconsin 53706

Received December 30, 1992. In Final Form: April 22, 1993

The attachment chemistry required for the sequential self-assembly of zirconium phosphonate (ZP) monolayers on gold and germanium surfaces is examined with a combination of attenuated total reflection (ATR-FTIR) and polarization modulation (PM-FTIR) Fourier transform infrared spectroscopies. On the germanium substrates, the conversion of an attached ω-aminosilane monolayer to phosphate amide species creates a primer for the sequential deposition of multilayer films of zirconium 1,10-decanediylbis(phosphonate) (Zr/DBP). On vapor-deposited gold films, a packed monolayer of 11-mercapto-1-undecanol (MUD) serves as the basis for a primer monolayer. PM-FTIR measurements show that phosphorylation of the terminal hydroxy groups results in a surface with a mixture of phosphate mono- and diesters, which bind Zr^{4+} to commence the self-assembly of the Zr/DBP multilayers. On both substrates, the alkyl chain regions of the ZP film are observed to be conformationally disordered due to the control of the lateral spacing in the films by the inorganic (phosphonate–Zr–phosphonate) regions. Furthermore, the packing density, order, and chemical structure of the primer layer are found to influence the resulting ZP multilayer structure.

Introduction

Organic thin films ranging in thickness from one monolayer to several hundred nanometers are currently employed in such diverse areas as optics, electronics, biotechnology, tribology, electrochemistry, and chemical sensors.[1,2] The versatility of these systems stems from the ease with which different chemical functionalities can be incorporated into the thin film in order to control the reactivity and molecular structure of the interface. One successful method for preparing thin organic films is the self-assembly of monolayers of alkanethiols[3,4] and silanes.[5,6] In 1988, T. E. Mallouk and co-workers at the University of Texas demonstrated the self-assembly of multilayer films onto metal and oxide substrates one monolayer at a time by the spontaneous adsorption and organization of zirconium alkyldiphosphonates.[7,8] A substrate was first primed with a monolayer of a phosphonate-terminated species, and then mixed organic/inorganic multilayers were prepared by the alternate exposure of the substrate to $ZrOCl_2$ and 1,10-decanediylbis(phosphonic acid) solutions (Figure 1). In contrast to other multilayers formed by spontaneous adsorption,[9] the sequential Zr^{4+}/phosphonate deposition process occurred with high reproducibility and efficiency. Ellipsometry and X-ray photoelectron spectroscopy (XPS) verified the sequential deposition of up to eight Zr/DBP monolayers. Subsequent papers by the Mallouk group have demonstrated that other organic molecules and inorganic ions could be incorporated into the ZP multilayers to create thin films useful in a variety of applications.[10–12]

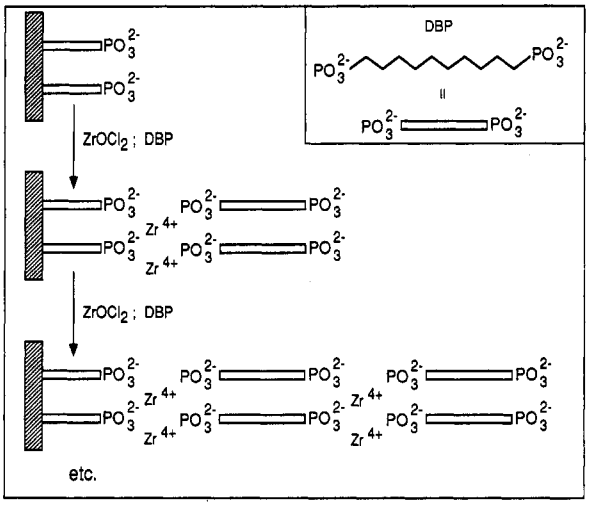

Figure 1. Schematic diagram of the Zr/DBP deposition process, first used by Mallouk et al.[8]

The formation of *oriented* ZP multilayers via an extension of the Mallouk deposition scheme was demonstrated by H. Katz, C. E. D. Chidsey, and co-workers at Bell Labs in 1990.[13,14] They prepared oriented multilayer films by the replacement of one of the phosphonate groups with a hydroxy group. After adsorption, the hydroxy group was phosphorylated (converted to a phosphate species) prior to the deposition of the next monolayer. Using this

(1) Swalen, J. D.; Allara, D. L.; Andrade, J. D.; Chandross, E. A.; Garoff, S.; Israelachvilli, J.; Mccarthy, T. J.; Murray, R.; Pease, R. F.; Rabolt, J. F.; Wynne, K. J.; Yu, H. *Langmuir* **1987**, *3*, 932–950.
(2) Ulman, A. *An Introduction to Ultrathin Organic Films*; Academic: New York, 1991.
(3) Dubois, L. H.; Nuzzo, R. G. *Annu. Rev. Phys. Chem.* **1992**, *43*, 437–463.
(4) Duevel, R. V.; Corn, R. M. *Anal. Chem.* **1992**, *64*, 337–342.
(5) Maoz, R.; Sagiv, J. *J. Colloid Interface Sci.* **1984**, *100*, 465–496.
(6) Wrighton, M. S. *Science* **1986**, *231*, 32–37.
(7) Lee, H.; Mallouk, T. E.; Kepley, L. J.; Hong, H. G.; Akhter, S. *J. Phys. Chem.* **1988**, *92*, 2597–2601.
(8) Lee, H.; Hong, H. G.; Mallouk, T. E.; Kepley, L. J. *J. Am. Chem. Soc.* **1988**, *110*, 618–620.
(9) Netzer, L.; Sagiv, J. *J. Am. Chem. Soc.* **1983**, *105*, 674.
(10) Akhter, S.; Lee, H.; Mallouk, T. E.; White, J. M.; Hong, H. G. *J. Vac. Sci. Technol., A* **1987**, *7*, 1608–1613.
(11) Cao, G.; Rabenberg, L. K.; Nunn, C. M.; Mallouk, T. E. *Chem. Mater.* **1991**, *3*, 149–156.
(12) Kepley, L. J.; Sackett, D. D.; Bell, C. M.; Mallouk, T. E. *Thin Solid Films* **1992**, *208*, 132–136.
(13) Putvinski, T. M.; Schilling, M. L.; Katz, H. E.; Chidsey, C. E. D.; Mujsce, A. M.; Emerson, A. B. *Langmuir* **1990**, *6*, 1567–1571.
(14) Katz, H. E.; Scheller, G.; Putvinski, T. M.; Schilling, M. L.; Wilson, W. L.; Chidsey, C. E. D. *Science* **1991**, *254*, 1485–1487.

0743-7463/93/2409-1815$04.00/0

strategy, they deposited oriented multilayers of dye molecules on a silica substrate, which exhibited a second harmonic generation (SHG) efficiency proportional to the square of the number of adsorbed monolayers. Oriented monolayers such as these have potential applications in both nonlinear optics and optoelectronics.

Thin organic films formed by the Langmuir–Blodgett (LB) dipping process are currently employed in a wide range of chemical and physical applications, despite occasional mechanical and thermal stability problems.[1,15] Since the ZP multilayers are formed by sequential spontaneous adsorption and organization, the resultant film structures should be more thermally stable and depend less upon the exact deposition conditions than LB films. In addition, spontaneous adsorption from solution lends itself to the formation of thin films on many unusual surfaces and geometries (e.g., optical fibers, mirrors, lenses), which are difficult to adapt to the LB dipping process. Thus, ZP multilayers may serve as a general alternative to the Langmuir–Blodgett technique of multilayer formation.[7]

However, before ZP multilayers gain a wide following for thin film formation, a number of questions remain about the molecular structure of the ZP multilayers: (i) How do molecular conformation and organization in the alkyl regions of the ZP multilayers compare with those of other organic thin films? (ii) Do the inorganic zirconium phosphonate layers control packing within the film, or do the organic regions control the film structure? (iii) To what extent does the primer layer influence the structure of the film? Can ZP monolayers with very high packing density be created by careful preparation of a primer layer with a high surface density of phosphonate or phosphate moieties?

To answer these questions about ZP films, we employ vibrational spectroscopy because it has been used quite successfully in the past as a probe of molecular structure in both self-assembled monolayers and LB films.[16–19] On Ge substrates, we monitor the buildup of a Zr/DBP multilayer on a phosphorylated aminosilane primer monolayer with attenuated total reflectance Fourier transform infrared (ATR-FTIR) spectroscopy. On vapor-deposited gold films, polarization modulation Fourier transform infrared (PM-FTIR) reflection–absorption spectroscopy[4,20–23] provides the submonolayer sensitivity required to follow the phosphorylation chemistry and Zr/DBP monolayer structure. A monolayer of self-assembled ω-hydroxyalkanethiols on Au serves as the basis for the formation of a densely packed primer monolayer. The PM-FTIR measurements show that phosphorylation converts the terminal hydroxy groups to a combination of phosphate mono- and diesters, which then function as a primer for the ZP multilayers.

(15) Gaines, G. L., Jr. *Immiscible Monolayers at the Liquid-Gas Interface*; Wiley: New York, 1966.
(16) Nuzzo, R. G.; Dubois, L. H.; Allara, D. L. *J. Am. Chem. Soc.* **1990**, *112*, 558–569.
(17) Tillman, N.; Ulman, A.; Penner, T. L. *Langmuir* **1989**, *5*, 101–111.
(18) McGarvey, C. E.; Holden, D. A.; Tchir, M. F. *Langmuir* **1991**, *7*, 2669–2676.
(19) Song, Y. P.; Yarwood, J.; Tsibouklis, J.; Feast, W. J.; Cresswell, J.; Petty, M. C. *Langmuir* **1992**, *8*, 262–266.
(20) Kunimatsu, K.; Golden, W. G.; Seki, H.; Philpott, M. R. *Langmuir* **1985**, *1*, 245–250.
(21) Golden, W. G. *Fourier Transform Infrared Spectrosc.* **1985**, *4*, 315.
(22) Dowrey, A. E.; Marcott, C. *Appl. Spectrosc.* **1982**, *36*, 414–416.
(23) Duevel, R. V.; Corn, R. M.; Liu, M. D.; Leidner, C. R. *J. Phys. Chem.* **1992**, *96*, 468–473.

Experimental Considerations

Materials. 11-Bromo-1-undecanol (Aldrich, 98%) was recrystallized from hexane. Water from a Millipore system was used throughout the experiments. Other solvents included absolute ethanol (Quantum) and UV grade acetonitrile (Burdick & Jackson). All other chemicals were used as received.

11-Mercapto-1-undecanol (MUD). MUD was prepared via the Bunte salt.[24] 11-Bromo-1-undecanol (1.25 g, 5.0 mmol) and sodium thiosulfate pentahydrate (Aldrich, 99.5%) (1.37 g, 5.5 mmol) were refluxed for 3 h in 50 mL of 1:1 ethanol–water. The solvent was removed by rotary evaporation, and the solid recrystallized from ethanol, yielding sodium 11-bromo-1-undecyl thiosulfate (1.35 g, 4.4 mmol), which was then refluxed in 100 mL of 6 M HCl for 6 h. The product was extracted with CH_2Cl_2; the extracts were washed with 4 M NaCl, dried with Na_2SO_4, and filtered. Rotary evaporation of the solvent left 11-mercapto-1-undecanol (0.45 g, 2.2 mmol): mp 30.5–31.5 °C; ^{1}H NMR ($CDCl_3$) δ 3.64 (t, 2H), 2.53 (q, 2H), 1.57 (m, 4H), 1.29 (m, 14H).

1,10-Decanediylbis(phosphonic acid). The synthesis by Mallouk et al. was used to prepare 1,10-decanediylbis(phosphonic acid) from 1,10-dibromodecane (Aldrich, 97%) and triethyl phosphite (Aldrich, 98%) with subsequent hydrolysis using HCl.[7] The product gave typical phosphonic acid bands in the IR (KBr pellet), and ^{1}H NMR showed a multiplet at δ 1.1–1.6.

Substrate Preparation and Primer Layer Formation. 1. Germanium. A germanium ATR crystal (Harrick, 50 × 10 × 3 mm, 60°, 17 reflections) was placed in fresh 80% H_2SO_4 (Fluka, puriss) for 8 h before rinsing with water and lightly polishing with 0.05-μm alumina (Buehler) to a mirror finish. The crystal was sonicated in water for 20 min, immersed into 80% H_2SO_4 for 5–10 h, thoroughly rinsed with water, and dried with N_2. A background spectrum was obtained at this point before deposition of the silane primer. The Ge ATR crystal was immersed into a 0.5% (v/v) solution of ω-aminosilane in boiling octane (Aldrich, 99+%) under nitrogen. The solution was refluxed for 18 h in the case of (4-aminobutyl)dimethylmethoxysilane (Huls America), but only 30 min for the (3-aminopropyl)trimethoxysilane (Aldrich, 97%). Removal of the crystal was followed by rinsing with octane, sonication in acetonitrile for 10 min, sonication in hot Millipore water for 10 min, thorough rinsing with water, and drying in a stream of nitrogen. The aminosilane monolayers were phosphorylated for 1 h in a solution of 0.2 M phosphorus oxychloride ($POCl_3$) (Aldrich, 99%) and 0.2 M 2,4,6-collidine (Aldrich, 99%) in dry acetonitrile under a N_2 atmosphere and then thoroughly rinsed with acetonitrile.

2. Gold. Vapor deposition of 1200 Å of Au (D.F. Goldsmith, 99.995%) onto clean glass microscope slide covers (Cida) was done using the apparatus described previously.[25] In lieu of the Cr adhesion layer, however, the glass was silanized with (3-mercaptopropyl)trimethoxysilane (Aldrich, 95%) in a manner similar to that reported by Majda et al.[26] A self-assembled monolayer was adsorbed onto the Au film from a 1 mM MUD solution in ethanol for 24–96 h and phosphorylated in the same manner as the aminosilane monolayers above.

Multilayer Deposition. Zr/DBP monolayers were formed atop the primer layer by alternate exposure to aqueous solutions of 5 mM zirconyl chloride octahydrate ($ZrOCl_2$) (Aldrich, 98+%) and 1.2 mM 1,10-decanediylbis(phosphonic acid) for 30 min (except where longer dipping times are noted). Between solutions, the substrate was thoroughly rinsed with a stream of water, immersed into pure water, and rinsed again with a water stream. Before obtaining an FTIR spectrum, the substrates were dried using a stream of nitrogen.

FTIR Measurements. All FTIR spectra were taken using a Mattson RS-1 spectrometer. At oxide and semiconductor surfaces, an attenuated total reflectance (ATR) geometry was employed with a wide-band HgCdTe detector. All ATR-FTIR background and sample spectra used a Spectra Tech Model 300 variable ATR holder to obtain 1024 scans at 4-cm^{-1} resolution. At gold surfaces, polarization modulation FTIR (PM-FTIR)

(24) March, J. *Advanced Organic Chemistry: Reactions, Mechanisms, and Structure*, 3rd ed.; John Wiley and Sons, Inc.: New York, 1985.
(25) Barner, B. J.; Corn, R. M. *Langmuir* **1990**, *6*, 1023–1030.
(26) Goss, C. A.; Charych, D. H.; Majda, M. *Anal. Chem.* **1991**, *63*, 85–88.

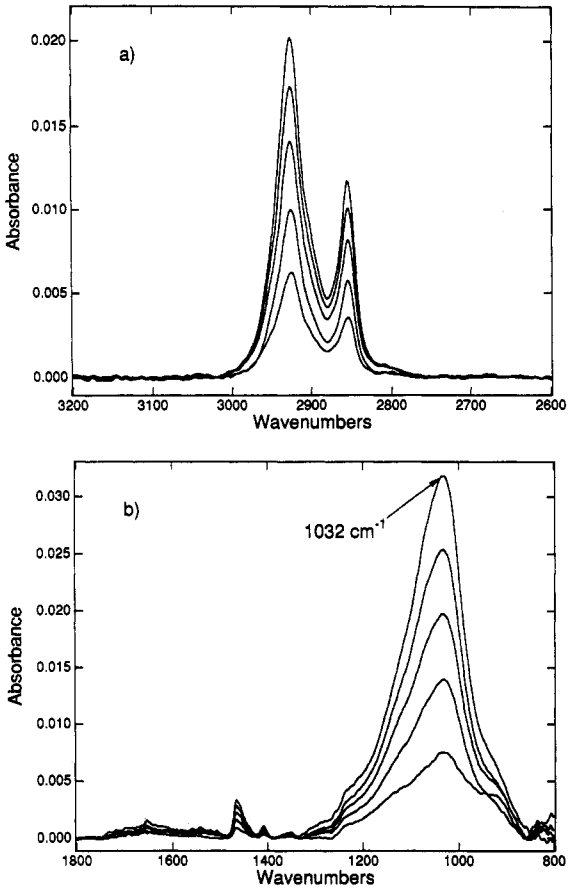

Figure 2. ATR-FTIR spectra of the first five Zr/DBP monolayers deposited onto a Ge substrate primed with a phosphorylated ω-aminosilane. (a) The CH stretching region shows asymmetric and symmetric methylene stretches at 2927 and 2854 cm^{-1}, respectively. (b) The mid-IR region exhibits CH_2 deformations at 1466 and 1410 cm^{-1}, and the asymmetric phosphonate stretch, $\nu_a(PO_3^{2-})$, at 1032 cm^{-1}.

differential reflectance measurements were obtained using the real-time interferogram sampling methods that were developed previously.[27] The optical layout followed that reported elsewhere:[27b] a ZnSe polarizer, a ZnSe photoelastic modulator, reflection off the sample at an angle of 77° from the surface normal, followed by a ZnSe lens and then the detector. For spectra in the CH stretching region, an InSb detector was employed to obtain spectra of 256–1024 scans at 2- or 4-cm^{-1} resolution. In the mid-IR region, a narrow-band HgCdTe detector was used to obtain spectra of 3000–5000 scans at 4-cm^{-1} resolution.

Results and Discussion

A. Zr/DBP Multilayer Formation on a Germanium Substrate. The CH stretching regions of the ATR-FTIR spectra for the first five Zr/DBP monolayers deposited onto a Ge ATR crystal are plotted in Figure 2a. The two bands at 2927 and 2854 cm^{-1} correspond to the asymmetric and symmetric methylene stretching modes, respectively, from the C_{10} alkyl chain of the DBP. These band positions indicate that the alkyl chains are not as conformationally ordered or as tightly packed as in crystalline *n*-decane or in a self-assembled monolayer of *n*-decanethiol on gold (i.e., the alkyl chains do not adopt a close-packed all-trans configuration).[28,29] Note that the band positions do not change with additional monolayers, indicating that the same structure is formed in each successive Zr/DBP layer. No dispersion effects were observed for any of the multilayers discussed in this paper. Dispersion effects were not seen for similar multilayer films and are not expected from complex Fresnel reflectance calculations on related model three-phase systems.[30,31] Furthermore, longer deposition times (*e.g.*, overnight) do not shift the band positions. The absence of a tightly packed array of alkyl chains suggests that the lateral interactions within the phosphonate–zirconium–phosphonate lattice define the monolayer structure, and that the alkyl chains remain conformationally disordered to accommodate the lateral spacing of the inorganic layer.

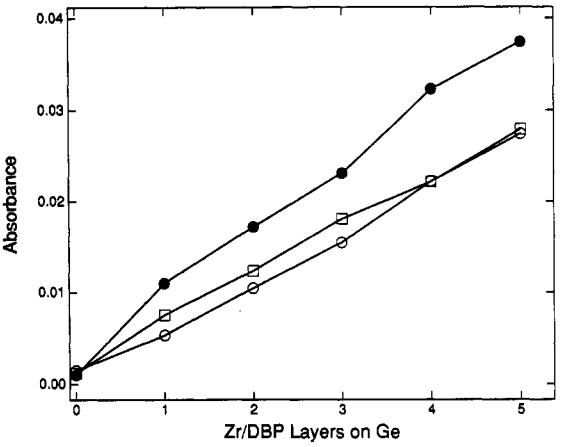

Figure 3. ATR-FTIR absorbance of the asymmetric CH_2 stretching mode at 2927 cm^{-1} as a function of the number of Zr/DBP monolayers deposited onto a Ge substrate with different primers: phosphorylated (3-aminopropyl)trimethoxysilane (solid circles), non-phosphorylated (3-aminopropyl)trimethoxysilane (open circles), and phosphorylated (4-aminobutyl)dimethylmethoxysilane (open squares). The points for zero Zr/DBP layers correspond to the absorbance of the primer layer.

The mid-IR regions of the ATR-FTIR spectra for the first five Zr/DBP monolayers deposited onto a Ge substrate are plotted in Figure 2b. Small methylene scissor deformation bands are observed at 1466 and 1410 cm^{-1}; the latter band corresponds to the CH_2 adjacent to the phosphonate group.[32,33] The strong asymmetric phosphonate stretch, $\nu_a(PO_3^{2-})$, at 1032 cm^{-1} dominates the spectrum,[34] and the intensity of this band increases linearly with each successive monolayer. The band position is close to that observed in bulk zirconium alkylphosphonates,[35] and does not change with the deposition of additional monolayers, although the band shape does vary slightly.

As mentioned in the Experimental Considerations, the Zr/DBP multilayers shown in Figure 2 are grown on a phosphorylated ω-aminosilane primer layer. The one- to two-monolayer primer film is formed by the reaction and polymerization of (3-aminopropyl)trimethoxysilane on the germanium oxide surface. Exposure of this film to $POCl_3$ converts the amino groups to phosphate amide moieties that can bind the first layer of Zr^{4+} ions. Figure 3 plots the intensity of the asymmetric methylene stretching band

(27) (a) Green, M. J.; Barner, B. J.; Corn, R. M. *Rev. Sci. Instrum.* **1991**, *62*, 1426–1430. (b) Barner, B. J.; Green, M. J.; Saez, E. I.; Corn, R. M. *Anal. Chem.* **1991**, *63*, 55–60.

(28) Snyder, R. G.; Strauss, H. L.; Elliger, C. A. *J. Phys. Chem.* **1982**, *86*, 5145–5150.

(29) Porter, M. D.; Allara, D. L.; Bright, T. B.; Chidsey, C. E. D. *J. Am. Chem. Soc.* **1987**, *109*, 3559–3568.

(30) Porter, M. D. *Anal. Chem.* **1988**, *60*, 1143.

(31) Swalen, J. D.; Rabolt, J. F. In *Fourier Transform Infrared Spectroscopy*; Ferraro, J. R., Basile, L. J., Eds.; Academic Press, Inc.: New York, 1985; Vol. 4.

(32) Bellamy, L. J. *The Infra-red Spectra of Complex Molecules*; Wiley: New York, 1975.

(33) Hayashi, S.; Unemura, J. *J. Chem. Phys.* **1975**, *63*, 1732.

(34) Socrates, G. *Infrared Characteristic Group Frequencies*; Wiley: Chichester, 1980.

(35) Hong, H. G.; Sackett, D. D.; Mallouk, T. E. *Chem. Mater.* **1991**, *3*, 521–527.

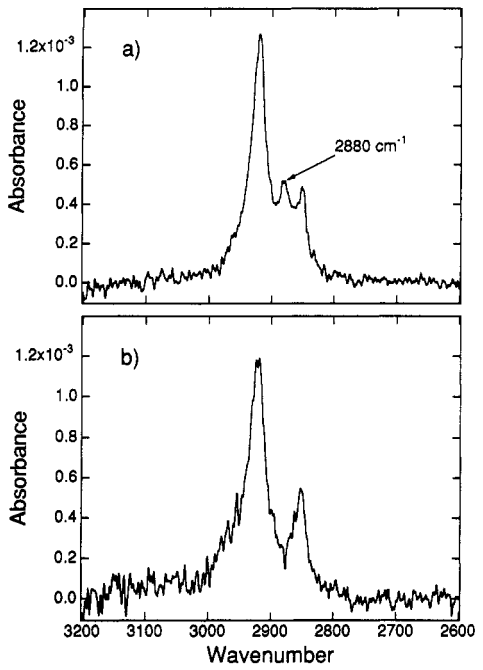

Figure 4. CH stretching region of the PM-FTIR spectra for a MUD monolayer on a vapor-deposited gold substrate: (a) before phosphorylation; (b) after phosphorylation. The 2880-cm^{-1} band is a methylene stretch of the CH_2 adjacent to the –OH group.

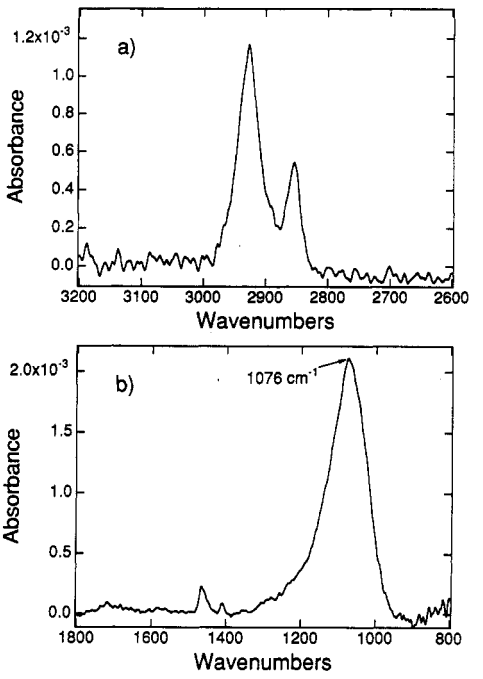

Figure 5. PM-FTIR spectrum of one Zr/DBP monolayer deposited onto a gold substrate coated with a phosphorylated MUD primer monolayer: (a) CH stretching region with asymmetric and symmetric methylene stretches at 2927 and 2854 cm^{-1}, respectively; (b) mid-IR region with CH_2 deformations at 1466 and 1410 cm^{-1}, and the asymmetric phosphonate stretch, $\nu_a(PO_3^{2-})$, at 1076 cm^{-1}.

at 2927 cm^{-1} as a function of the number of Zr/DBP layers on this primer (solid circles). The intensity rises monotonically with an average increase of 4.2×10^{-4} absorbance units per monolayer (after accounting for the 17 reflections in the ATR crystal). A smaller absorbance is observed if the primer monolayer does not undergo phosphorylation before Zr^{4+} deposition (the open circles in Figure 3). Apparently, the surface amino groups can also bind Zr^{4+} ions, but to a lesser extent.

A lower surface density of phosphate amide groups can be prepared via the phosphorylation of a primer monolayer formed by the reaction of (4-aminobutyl)dimethylmethoxysilane with the germanium surface. This silane's inability to cross-link and its methyl groups reduce the amino group surface concentration, as verified by ATR-FTIR measurements. The absorbance per Zr/DBP layer formed on this primer is plotted in Figure 3 (open squares), and is much less than for the more densely packed trimethoxysilane primer layer. Thus, a more tightly packed ω-aminosilane primer increases the packing density of the Zr/DBP monolayers.

B. Zr/DBP Multilayer Formation on a Gold Substrate. The observed sensitivity of the Zr/DBP film structure to the silane primer layer suggests that more ordered ZP multilayers might form on substrates with a well-defined, ordered primer monolayer. For example, on gold surfaces an ordered monolayer of self-assembled ω-hydroxyalkanethiols has been used previously.[13,36-38] Phosphorylation of this primer is thought to yield a packed layer of phosphate esters. Figure 4a depicts the PM-FTIR spectrum (CH stretching region) of a monolayer of 11-mercapto-1-undecanol (MUD) self-assembled onto a vapor-deposited gold film. The band at 2880 cm^{-1} has been identified previously as a CH_2 stretching mode from the terminal $-CH_2OH$ group.[16,32,39] Upon phosphorylation of this monolayer with $POCl_3$, the frequency of this mode shifts[32] and this band disappears (Figure 4b). The loss of the 2880-cm^{-1} band verifies the conversion of the terminal alcohol groups to phosphate ester species.

The asymmetric and symmetric CH_2 stretching bands for the MUD monolayer occur at 2919 and 2850 cm^{-1} both before and after phosphorylation. These frequencies indicate a well-ordered and tightly packed monolayer on the gold surface.[39] This phosphorylated MUD monolayer acts as a primer for the Zr/DBP monolayer whose infrared spectrum is shown in parts a and b of Figure 5, CH and mid-IR regions, respectively. Unfortunately, the CH stretching region of the Zr/DBP monolayer shows that the DBP alkyl chains do not adopt the tight packing behavior of the primer. Instead, they exhibit the same CH_2 stretching frequencies (2927 and 2854 cm^{-1}) observed for the ZP multilayers on Ge (Figure 2a); this reaffirms the previous conclusion that the inorganic regions control the lateral spacing of these films.

The mid-IR region of the PM-FTIR spectrum of a Zr/DBP monolayer (Figure 5b) is dominated by the asymmetric phosphonate stretch, $\nu_a(PO_3^{2-})$, at 1076 cm^{-1}. This phosphonate band reproducibly differs by more than 40 wavenumbers from the phosphonate band position observed in the bulk spectrum and in the Zr/DBP monolayers deposited onto the germanium substrate (Figure 2b). The shift of this band denotes a different structure of the zirconium phosphonate lattice on the MUD primer layer from that on the silane primers.

To investigate the variability of the $\nu_a(PO_3^{2-})$ band position, a slightly different primer layer is formed by reacting (3-aminopropyl)trimethoxysilane with the terminal hydroxy groups of an ordered MUD monolayer on gold.[36] Phosphorylation of the amino groups and subse-

(36) Ulman, A.; Tillman, N. *Langmuir* **1989**, *5*, 1418–1420.
(37) Bain, C. D.; Biebuyck, H. A.; Whitesides, G. M. *Langmuir* **1989**, *5*, 723–727.
(38) Miller, C.; Cuendet, P.; Grätzel, M. *J. Phys. Chem.* **1991**, *95*, 877–886.
(39) Chidsey, C. E. D.; Loiacono, D. N. *Langmuir* **1990**, *6*, 682–691.

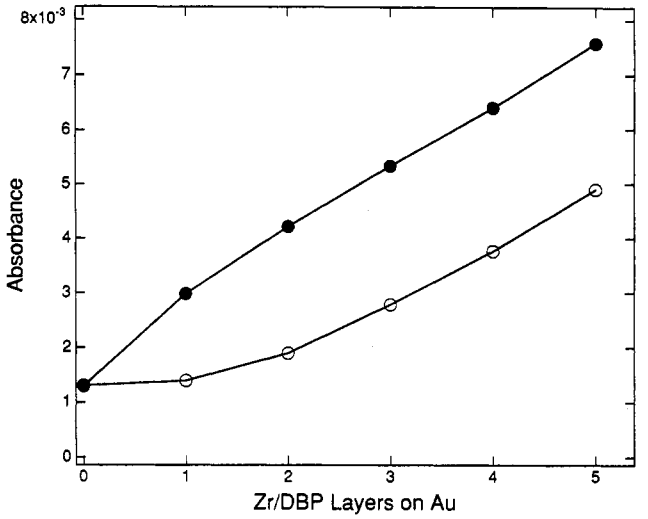

Figure 6. Intensity of the asymmetric CH_2 stretching mode at 2927 cm^{-1} as a function of the number of Zr/DBP monolayers deposited onto a Au substrate with a phosphorylated MUD primer monolayer (solid circles), and a non-phosphorylated MUD monolayer (open circles). The data points for zero Zr/DBP layers correspond to the absorbance of the primer layer.

quent Zr/DBP deposition results in a PM-FTIR spectrum with the $\nu_a(PO_3^{2-})$ band near 1065 cm^{-1}—between the 1076 cm^{-1} observed using the MUD primer alone on Au and the 1032 cm^{-1} observed with the trimethoxysilane primer on Ge. This intermediate band position suggests that the MUD layer has changed the ω-aminosilane primer layer (by imposing order and/or increasing its surface density). A change in the surface concentration of amino groups changes the density of phosphate groups, which could then affect the positioning of Zr^{4+} ions and ultimately the zirconium phosphonate crystal structure. Therefore, the packing density of the primer (hydroxythiol or aminosilane) influences the ZP multilayer structure, as evidenced by the large variability of the Zr/DBP phosphonate band position with different primers.

The absorbance of the CH_2 stretching band at 2927 cm^{-1} as a function of the number of Zr/DBP monolayers deposited onto the gold surface primed with a phosphorylated MUD monolayer is shown in Figure 6 (solid circles). The intensity rises in a nearly linear fashion with an average increase of 1.25×10^{-3} absorbance units per monolayer. An enhancement of approximately 3.5 is expected for the intensity of the infrared electromagnetic fields at a gold surface in a reflection geometry at an angle of incidence of 77°.[30] In accordance with this enhancement, we observe on gold surfaces an absorbance per Zr/DBP monolayer of 1.25×10^{-3}, which is about 3 times the value observed at a Ge surface in section A. The additional surface roughness of the Ge sample is probably responsible for the difference between the calculated value of 3.5 and the observed value of 3. The Zr/DBP multilayer buildup on a *non*-phosphorylated MUD primer is also shown in Figure 6 (open circles). Apparently, a small amount of adsorption occurs due to interaction of the Zr^{4+} with the OH groups. Unlike the non-phosphorylated aminosilane primer layers, the amount of DBP deposited onto the MUD starts off very low and then the film "self-anneals" to the point where the intensity change per monolayer eventually equals that observed for the phosphorylated MUD primer.

C. Phosphorylation Chemistry of the MUD Monolayer. Since phosphorylation significantly affects at least the first few ZP layers and it plays a key role in the formation of oriented multilayers, the chemical steps involved in the formation of surface phosphate ester species

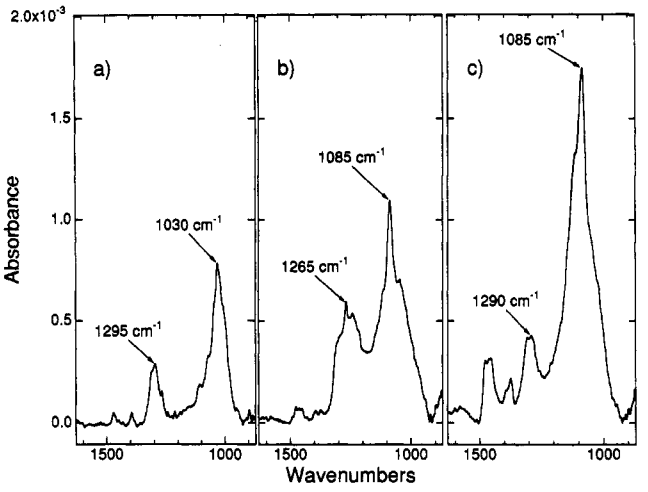

Figure 7. Mid-IR region of the PM-FTIR spectra for a MUD monolayer on a vapor-deposited gold substrate: (a) after exposure to $POCl_3$ in acetonitrile; (b) after dipping in water; (c) after exposure to a $ZrOCl_2$ solution. See Table I and the text for assignment of the phosphate stretching bands.

Table I. Infrared Frequencies and Vibrational Assignments for the Phosphate Bands in Figure 7[32,34,40-42]

	frequency (cm^{-1})	assignment	species
Figure 7a	1295	ν(P=O)	1, 2
	1030	ν(P—O—(C))	1, 2
Figure 7b	1290 shoulder	$\nu_a(PO_2^-)$	5, 6
	1270–1240	ν(P=O) (hydrogen-bonded)	3, 4
	1085	ν(P—O—(C))	3–7
		$\nu_s(PO_2^-)$	5, 6
		$\nu_a(PO_3^{2-})$	7
Figure 7c	1290	$\nu_a(PO_2^-)$	6
	1085	ν(P—O—(C))	6, 7
		$\nu_s(PO_2^-)$	6
		$\nu_a(PO_3^{2-})$	7

were investigated in depth. Figure 7 shows a series of PM-FTIR spectra at various stages of the reaction of the surface hydroxy groups, and Table I gives the phosphate band assignments.[32,34,40-42] Immediately after exposure to a $POCl_3$ solution and thorough rinsing with dry acetonitrile, the PM-FTIR spectrum in Figure 7a is obtained. Two phosphate bands are observed: a P—O—(C) stretch at 1030 cm^{-1} and a P=O stretch at 1295 cm^{-1}. These two phosphate bands result from the two possible phosphorochloridate species 1 and 2 that exist on the surface:

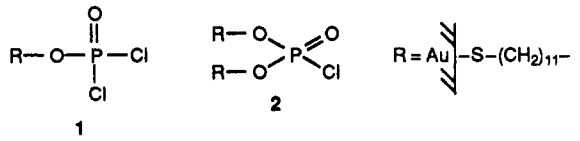

where R represents the alkyl chain of the MUD monolayer on gold. We have neglected the possibility of phosphate triester species for steric reasons, and because a significant number of triesters would not result in the observed ZP buildup. The appearance of these phosphate bands along with the loss of the 2880-cm^{-1} CH_2 stretching band

(40) Lin-Vien, D.; et al. *The Handbook of Infrared and Raman Characteristic Frequencies of Organic Molecules*; Academic: Boston, 1991.

(41) Thomas, L. C. *Interpretation of the Infrared Spectra of Organophosphorus Compounds*; Heyden: London, 1974.

(42) (a) Thomas, L. C.; Chittenden, R. A. *Spectrochim. Acta* **1964**, *20*, 467–487. (b) Thomas, L. C.; Chittenden, R. A. *Spectrochim. Acta* **1964**, *20*, 489–502. (c) Thomas, L. C.; Chittenden, R. A. *Spectrochim. Acta* **1970**, *26A*, 781–800.

(mentioned in the previous section) indicates that the MUD hydroxy groups have been converted to species 1 and 2.

After dipping the gold surface in water, the spectrum changes to that plotted in Figure 7b. Now the phosphate bands arise from five possible ester moeities: two neutral species, 3 and 4

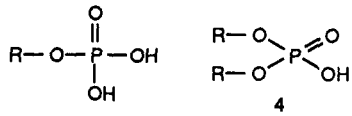

3 4

and three charged species, 5–7

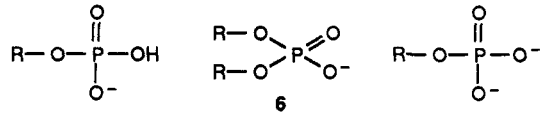

5 6 7

Both phosphate bands grow in intensity as compared to those in Figure 7a. The P=O band is broader and more complex, with the band center shifting from 1295 to 1265 cm^{-1}. This band now contains the hydrogen-bonded P=O stretch of the two neutral species 3 and 4 in the region 1270–1240 cm^{-1}, and the asymmetric PO_2^- stretch, $\nu_a(PO_2^-)$, of species 5 and 6 appearing as a shoulder at 1290 cm^{-1}. The other phosphate band moves from 1030 to 1085 cm^{-1}, and it is now a combination of (i) the P—O—(C) stretch of all five species, (ii) the symmetric PO_2^- stretch, $\nu_s(PO_2^-)$, of species 5 and 6, and (iii) the asymmetric PO_3^{2-} stretch, $\nu_a(PO_3^{2-})$, of species 7 (if any exists at this neutral pH). Both phosphate bands have broad and sharp components; we attribute the broad components to the hydrogen-bonded species on the surface.

Exposure of the surface to a $ZrOCl_2$ solution for 30 min results in the spectrum depicted in Figure 7c. Exposure to $ZrOCl_2$ for up to 2 days produced no change in this spectrum. The complexation of the Zr^{4+} ions with the surface phosphate groups should convert the P—OH species to anions, leaving a surface with only the phosphate mono- and diesters 6 and 7. This conversion does occur, as verified by the changes in the broad 1265-cm^{-1} band, which loses intensity, narrows, and shifts to 1290 cm^{-1}. This band is due solely to $\nu_a(PO_2^-)$ of species 6, the phosphate diester, since the hydrogen-bonded P=O no longer exists and the PO_3^{2-} of species 7 has no absorption in this region. In contrast, the band at 1085 cm^{-1} significantly increases in intensity due to (i) the sharpening of the P—O—(C) stretch in the absence of hydrogen bonding, (ii) an increase in $\nu_s(PO_2^-)$ from the conversion of species 4 to species 6, and (iii) an increase in $\nu_a(PO_3^{2-})$ from the formation of species 7 from species 3 and 5.

The presence of $\nu_a(PO_2^-)$ at 1290 cm^{-1} in Figure 7c demonstrates that the primer monolayer must contain some phosphate diesters (species 6). However, phosphate monoesters (species 7), exist as well, as shown by the large increase of the 1085-cm^{-1} band without a concomitant increase in the 1290-cm^{-1} band upon complexation with Zr^{4+} (Figure 7b to 7c). This uncoupled increase in the 1085-cm^{-1} band must be due, at least in part, to $\nu_a(PO_3^{2-})$ of the phosphate monoester. Similar results were obtained by Bertilsson and Liedberg.[43]

Summary and Conclusions

In this paper the effect of the surface primer layer attachment chemistry on the spontaneous adsorption of monolayers and multilayers of zirconium phosphonates has been examined with a combination of ATR-FTIR and PM-FTIR spectroscopies. On germanium surfaces, the primer obtained by conversion of an aminosilane monolayer to phosphate amide species yields Zr/DBP multilayer films with some conformational disorder in the C_{10} alkyl chains. The amount of this conformational disorder does not change as a function of the number of monolayers deposited onto the surface. Furthermore, the density of phosphate amide species in the primer controls the surface packing density of the Zr/DBP film. On gold surfaces, phosphorylation of an ω-hydroxy-*n*-alkanethiol monolayer forms a highly packed primer surface. PM-FTIR spectra show that phosphorylation of the terminal hydroxy groups results in a mixed monolayer of phosphate mono- and diesters. The high surface concentration of phosphate species on the gold surfaces does not change the amount of conformational disorder in the C_{10} alkyl chains (organic regions) of the Zr/DBP layers, but it does alter the zirconium–phosphonate lattice structure (inorganic regions) as compared to Zr/DBP multilayers formed on the less densely packed phosphorylated ω-aminosilane primers deposited on both Ge and modified Au surfaces. In future PM-FTIR experiments, we will examine changes in film structure from incorporation of different organic functionalities into the ZP multilayers, and we will apply the technique of optical second harmonic generation[44] to ascertain the average molecular orientation of nonlinear active organic groups within the ZP multilayer films.

Acknowledgment. The authors gratefully acknowledge the support of the National Science Foundation in these studies. B.L.F. especially wishes to thank the NSF for a graduate research fellowship. We also thank Mattson Instruments for the RS-1 spectrometer on which all of the FTIR measurements were performed, and Steve Weibel at Mattson Instruments for his help in setting up the PM-FTIR apparatus.

(43) Bertilsson, L.; Liedberg, B. *Langmuir* **1993**, *9*, 141–149.
(44) Higgins, D. A.; Abrams, M. B.; Byerly, S. K.; Corn, R. M. *Langmuir* **1992**, *8*, 1994–2000.